Applied Environmental Research
- RESEARCH FOR SUSTAINABLE PLANET -

Research Article

Use of Modified Blast Furnace Slag for Cadmium Removal in An Aqueous Medium

Toufik Chouchane[1,*], Mohamed Tayeb Abedghars[1], Sabiha Chouchane[2], Hazem Meradi[1], Atmane Boukari[1]

[1] *Research Center in Industrial Technologies CRTI, Cheraga 16014 Algiers, Algeria*
[2] *Faculty of Sciences, Badji Mokhtar University, Annaba, Algeria*

*Correspondence Email: chouchane_toufik@yahoo.fr

Abstract

In this work, blast furnace slag was converted to hydroxyapatite-zeolite (MS) through alkaline fusion and hydrothermal treatment, and then it was used to remove cadmium in solution by adsorption in batch mode. The process was accomplished under the influence of determining parameters, namely the contact time, mass of the adsorbent, stirring speed, pH of the medium, temperature of the solution, particle size of the slag, and initial concentration. MS consists mainly of sodium oxide, silica, alumina, lime, and phosphorus pentoxide. The Ca/P, Na/Al, and Si/Al ratios revealed that the converted slag is a hydroxyapatite-zeolite. Following the modification of the treated slag, the specific surface area increased from 282.5 to 410.23 ml g^{-1}. Its zero charge point was detected at pH 3.2. After 50 min, the test results revealed that equilibrium was established. Furthermore, they demonstrated that the adsorption capacity was maximum (133.34 mg) at a pH of 6, at a temperature of 25 °C, at a stirring speed of 200 rpm, at a solid mass of 1g, at a particle size of 300 µm, and at an initial concentration of 240 mg L^{-1}. Exploration of the adsorption isotherms revealed that the Langmuir model better presented the adsorption process, thus revealing that the adsorption occurred on a monolayer surface. The parameters of the examined models, namely RL and n, affirmed that the adsorption is favorable. The kinetic study revealed that this process agreed more with the pseudo-second-order kinetic model, and the transport of pollutant is ensured by external and intraparticle diffusion. Thermodynamic analysis has shown that this process is spontaneous, exothermic, less entropic, and performed under physical interactions. The desorption process revealed that the reuse of MS is possible over five cycles with hydrochloric acid as an eluent. This study opens up advantageous perspectives for the sorption of cadmium from water.

ARTICLE HISTORY

Received: 21 Dec. 2023
Accepted: 20 May 2024
Published: 27 Jun. 2024

KEYWORDS

Adsorption;
Cadmium;
Kinetics;
Slag;
Zeolite

Introduction

Cadmium is an extremely harmful element and can accumulate in bodies, leading to terrible consequences for human health such as hypertension, calcium loss, kidney failure, a reduction in red blood cells, brain dysfunction, and damage bone marrow and nervous system [1]. This is why it was classified by the World Health Organization and the International Agency for Research on Cancer as one of the most dangerous pollutants [2]. In order to remedy this disaster, effective innovative techniques have been developed, namely membrane separation, ion exchange, electro-chemical treatment, chemical precipitation, adsorption, coagulation flocculation, and filtration [1, 3–4]. According to literature statements, it has been reported that the adsorption process is the most effective given its simplicity and reliability. In addition, it is economical, regenerates less sludge and consumes less energy [1, 3]. It is with this in mind that we attempted to incorporate a derivative of blast furnace slag, more precisely zeolite, in the process of removing cadmium by adsorption in batch mode.

https://doi.org/10.35762/AER.2024027

It should be mentioned that various research has been carried out on the adsorption process of cadmium in solution. Effectively, it has only been noticed that multiple adsorbents such as Biocher (CIB500) [5], thermally activated sepiolite [6], activated carbon from agricultural biomass [7], pinus halepensis sawdust [8], modified zeolite-supported zero- valence iron composites [9], graphene on TiO_2 nanofibers [10] and layered double hydroxide nanoparticles immobilized on iron slag [11], were used to eliminate cadmium in solution by adsorption phenomenon.

The examined zeolite was prepared from treated blast furnace slag. This by-product is generated during the production of cast iron at a percentage varying from 20 to 35%. Its annual global production is around 350 million tons, which represents a considerable economic loss. In addition, it can pollute water, air, and soil since it is constantly stored in the open air. Initially, it was introduced into road filling and construction material manufacturing [12]. Recently, it has been introduced into the manufacturing of cement, ceramics, agricultural fertilizers, and wastewater treatment products [6]. In the latter case, our team made a slight contribution by exploiting the slag as an adsorbent in the process of elimination of nickel, lead, manganese, copper, and trivalent chromium [13–17]. These research works were accomplished in order to valorize slag in the field of water depollution, specifically in the removal of metal ions in solution.

In order to give more scale to the slag in the adsorption processes, that is to say, to expand its specific surface area and thus increase its adsorption capacity, we proceeded to convert the slag into zeolite (MS). The experimental approach was based on the chemical and thermal activation of the slag samples, which were treated in several stages.

According to literature data, the exploitation of steel slag derivatives in the adsorption process has been cited in various research works. For example, prepared zeolite and silica from blast furnace slag were used in the adsorption process of methylene blue in solution [18–19]. Based on this research, the adsorption capacity of MB by zeolite and silica was reported to be 21.89 and 109.8 mg g^{-1}, respectively. It has also been mentioned that metaettringite synthesized from blast furnace slag, oxalated blast furnace slags, and hydrated calcium silicates derived from slags have been exploited in the adsorption processes of boron, cobalt, and other toxic metals, respectively [20–22]. The adsorbed amount of boron on synthesised metaettringite was 118.9 mg g^{-1}, and the maximum adsorbed amount of cobalt on oxalated blast furnace slag was 576 mg g^{-1} [20–21]. However, the maximum adsorption capacities for various heavy metals on hydrated calcium silicates all exceed 100 mg g^{-1} [22]. In the same context, basic slag from modified oxygen furnaces was used for the adsorption of dyes and copper in solution, separately [23–24]. The adsorbed amounts of reactive red 120, reactive blue 19, and reactive black 5 on treated oxygen furnace basal slag were 55, 60, and 76 mg g^{-1}, respectively [23]. In addition, the adsorption rate of copper on oxygen furnace-treated basal slag reached 99.9% [24]. It is important to mention that bibliographic data in direct relation to our work indicated that blast furnace slag successfully converted to hydroxyapatite-zeolite was used in the adsorption processes of manganese, ammonium, and phosphate ions. The same source indicated that the adsorption of manganese, ammonium, and phosphate ions in an initial solution of 50 mg L^{-1} was 25.98, 20.10, and 26.41 mg g^{-1}, respectively [25].

The main objective of this research was to convert blast furnace slag into zeolite to improve its adsorbent capacity. Second, to demonstrate its performance as an adsorbent in wastewater containing cadmium. In this work, the structure of the treated and modified slag was examined using X-ray fluorescence (XRF) and X-ray diffraction (XRD), and its specific surface area was defined by the Brunauer, Emmett et Teller model (BET model). The contact time, stirring speed, dosage of the adsorbent, pH of the medium, temperature of the medium, particle size of the solid, and initial concentration of the solution were used to improve and optimize this process. The interaction between MS and cadmium was explained by adsorption isothermal models specific to adsorption processes, namely Freundlich, Langmuir, and Temkin models. The kinetics of cadmium adsorption were studied using pseudo-first-order, pseudo-second-order, and diffusion models. The thermodynamic study made it possible to determine the nature of this process. The desorption process was examined using different eluents and distilled water.

Materials and methods

1) Treatment of adsorbent

The slag from the blast furnace used was treated according to the experimental protocol defined by Chouchane et al. [13–17]. Based on the research conducted [14, 26–28], we sought to transform slag from the blast furnaces treated into zeolite, minimizing lime content and increasing silica and alumina content. The operating protocol undertaken in this experimental phase is represented as follows:

Initially, we proceeded to prepare a solution in a one-liter beaker by adding 50 g of treated slag and NaOH at a concentration of 1 M. The solution was

heated to a temperature of 80 °C and stirred at a speed of 200 rpm for a period of 4 h. The mixture was left to stand for 2 h, then heated to 850 °C for a period of 120 min. After that, Na_2HPO_4 solution at a concentration of 10 mg L^{-1} was added and mixed at a moderate speed of 100 rpm until homogeneous. The homogenized solution was gradually enriched with drops of NaOH over a period of 5 min, after which it was allowed to stand until the solid and liquid were completely separated. After being recovered by filtration and cleaned with distilled water, the solid was steamed at 105 °C for 12 h before being stored in plastic boxes.

2) Reagents and materials

The cadmium ions were assayed by atomic absorption spectrometry (Perkin Elmer 3110). The characterization of the solid samples was carried out by X-ray fluorescence (Siemens SRS 3000) and X-ray diffraction (Rigaku Ultim IV). The pH of the solution was measured by a pH meter (Ericsson). Heating of the adsorbent was carried out by a muffle furnace (Nabertherm HT16/17). Stirring was carried out using a mechanical stirrer operating at different speeds. The specific surface of the slag samples was measured using the Brunauer, Emmett and Teller model (BET model).

3) Specific surface area determination

The specific surfaces of the treated slag samples and the zeolite were determined from the quantity of nitrogen adsorbed as a function of its pressure. This process was carried out at the boiling temperature of liquid nitrogen (-196 °C) and under normal atmospheric pressure (760 mmHg) [2]. The experimental data of N2 gas desorption at 77K were evaluated with the BET model [29].

4) Adsorption process

Batch mode experiments were performed to examine the adsorption of cadmium on the zeolite. The tests were carried out using solutions of volume 1 liter. The technical approach is to introduce a very precise quantity of MS into a solution containing cadmium of known concentration prepared from cadmium salt ($Cd(NO_3)_2{\cdot}4H_2O$). The experimental procedure was inspired by the method recommended by Chouchane et al. [13]. The experimental conditions applied in this process are described as follows:

In this study, we first analyzed the impact of contact time with the aim of optimizing the number of tests performed. The influence of contact time was studied for a period ranging from 0 to 180 min, under specific conditions: C_0: 30 mg L^{-1}, $V_{ag.}$: 100 rpm, pH: 4.8, T: 20 °C, IIIs: 400 µm, m_s: 1g. On the other hand, the effects of the mass of the adsorbent (m_s), the stirring speed (V_{ag}), the pH of the solution (pH), the particle size of the solid (IIIs), the concentration initial of the solution (C_0), and the temperature of the medium (T) were examined over a period ranging from 0 to 50 minby varying their values. The mass of the adsorbent (m_s) was studied from 0.2 to 1.4 g (0.4, 0.6, 0.8, 1, 1.2, and 1.4 g). The stirring speed (V_{ag}) was operated between 50 and 200 rpm, including speeds of 50, 100, 150, and 200 rpm. The pH of the solution was adjusted between 2.8 and 6.5, with specific values of 2.8, 4.4, 4.8, 6, and 6.5. The particle size of the solid (IIIs) was varied from 200 to 500 µm (200, 300, 400, and 500 µm). The initial concentration of the solution (C_0) was examined from 30 to 300 mg L^{-1} (30, 60, 90, 120, 150, 180, 210, 240, 270, and 300 mg L^{-1}). The temperature of the medium (T) was studied between 20 and 55 °C (20, 35, 45, and 55 °C).

The adsorbed quantity of cadmium (q_e) and the adsorption percentage (R) are calculated from Eq. 1 and 2.

$$q_e = \frac{C_0 - C_t}{m_s} \times V \qquad \text{(Eq. 1)}$$

$$\%R = \frac{C_0 - C_e}{C_0} \times 100 \qquad \text{(Eq. 2)}$$

Where: C_0: initial solution concentration, (mg L^{-1}), C_t: solution concentration after a time t (mg L^{-1}); C_e: Concentration at equilibrium (mg L^{-1}), V: volume of the solution (L) and m_s: adsorbent mass (g).

5) Point of zero charge

The approach developed by Chouchane et al. [14] was used to define the zero charge point (PZC). For this experiment, we used 2 g of adsorbent in 0.1 and 0.01 N potassium chloride (KCl) solutions for each test. The purpose of these tests was to identify the type of adsorbent burden. Indeed, the pH_{pzc} value tells us about the nature of the adsorbent surface. If the pH is greater than pH_{pzc}, it is negative, which facilitates cationic adsorption. Otherwise, it promotes anionic adsorption [3].

6) Desorption process

The method advocated by Chouchane et al. [16–17] was followed in the desorption of cadmium ions from modified slag (MS). The following experimental methodology was used to carry out this action:

• Using filter paper, 10 g of saturated adsorbent were obtained.

• The recovered MS was dehydrated for 24 h at 105°C.

• Cadmium desorption was carried out using H_2O and several eluents, namely HCL, H_2SO_4 and HNO_3, at a concentration of 0.1M.

• The desorption process was completed after 80 min of agitation (150 rpm).

• All tests were conducted in beakers of 1 L volume.

Results and discussion

1) Characterization of adsorbent

The results of solid characterization tests performed by XRF and XRD are presented in Tables 1 and Figure 1, respectively.

According to Chouchane et al. [14], it was indicated that slag consists mainly of silica (SiO_2: 40.1%) lime (CaO: 35.45%), alumina (Al_2O_3: 12.96%) and magnesium oxide (MgO: 5.12%) (Table1 and Figure 1a). On the other hand, analyzes of zeolite revealed that it is composed of mainly of sodium oxide (Na_2O: 27,11%), silica (SiO_2: 20,74%), alumina (Al_2O_3: 15,78%), lime (CaO: 11.65%), and phosphorus pentoxide (P_2O_5: 7.28%), (Table 1). The rise in sodium oxide percentage from 0.7 to 27.11% indicated that the conversion of BFS to MS was successfully completed. Additionally, the presence of phosphorus pentoxide was observed in the final product. It is essential to specify that LOI is an expression equivalent to the loss of mass detected during the analysis of the solid samples examined.

Table 1 Chemical composition of treated slag (BFS) [14] and modified slag (MS)

Elements	Mass %	
	BFS	MS
CaO	35.45	11.64
Al_2O_3	12.96	15.78
SiO2	40.1	20.74
Fe_2O_3	2.11	0.82
MgO	5.12	1.02
MnO	1.04	0.4
K_2O	0.2	0.21
Na_2O	0.7	27.11
P_2O_5	0	7.27
LOI	2.32	14.98

Physico-chemical tests carried out by XRD had confirmed the results carried out by XRF. Indeed, it has been observed that MS is essentially composed of sodium oxide, silica, alumina, lime, and phosphorus pentoxide (Figure 1b). It is important to mention that the absence of minor metal ions is due to their dispersion in the MS structure [28]. The Ca/P, Na/Al and Si/Al ratios are 1.61, 1.71 and 1.31, respectively. From these results, we were able to conclude that modified slag (MS) is essentially composed of zeolite (Na_2O, SiO_2, Al_2O_3) and hydroxyapatite (P_2O_5, CaO) [30–31].

2) Effect of contact time

The influence of the contact time on the adsorption of the pollutant in solution is crucial because it allowed us to reduce the duration of the tests and to determine the time of thermodynamic pseudo-equilibrium. The effect of contact time from 0 to 180 min is shown in Figure 2a. The experimental data clarified that the cadmium adsorption by MS achieves thermodynamic equilibrium after 50 min of contact under the aforementioned experimental requirements (Figure 2a). Furthermore, it was noted that the adsorption went through three phases: fast (0 at 30 min), weak (30 at 50 min), and inactive from 50 min. The speed of the process was prompted by the presence of multiple free sites on the adsorbent surface [6]. The attractive forces existing between the cadmium ions and the adsorption sites contributed positively to this outcome. The low adsorption was caused by the gradual reduction of free adsorption sites. Moreover, the cessation of the adsorption process was due to the unavailability of vacant adsorption sites and, consequently, saturation of the adsorption surface [17]. From literature, it was noticed that the adsorption of cadmium on different adsorbents, namely kaolinite, empty palm fruit clusters, magnetic biochar, and manganese-modified biochar has been accomplished after 120.9 min, 90 min, 30 min, and 6 h, respectively [30–33]. Based on this result, we could conclude that the adsorption of cadmium on MS was rather rapid.

3) Effect of adsorbent dosage

The influence of adsorbent dose on cadmium adsorption by MS is illustrated in Figure 2b. According to the tests performed, it was noted that at doses of adsorbent between 0.4 and 1 g L^{-1}, the efficiency and sorption capacity of cadmium increased by 48.88% and 14% respectively (Figure 2b). On the other hand, we observed that at $m_s > 1$g the adsorption rate and capacity decreased by 9.75% and 2.92 mg g^{-1}. The multiplication of free adsorption sites was undeniably responsible for the efficiency of cadmium adsorption on MS [34]. The reduction in adsorption efficiency is probably generated by the insufficiency of cadmium ions supplied relative to the growing active adsorption sites [35].

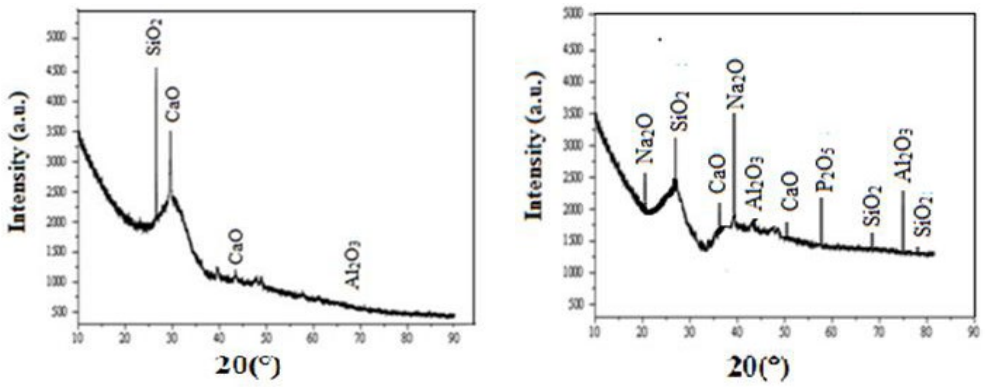

Figure 1 Diffractogram (a) slag (BFS) [16] and (b) modified slag (MS).

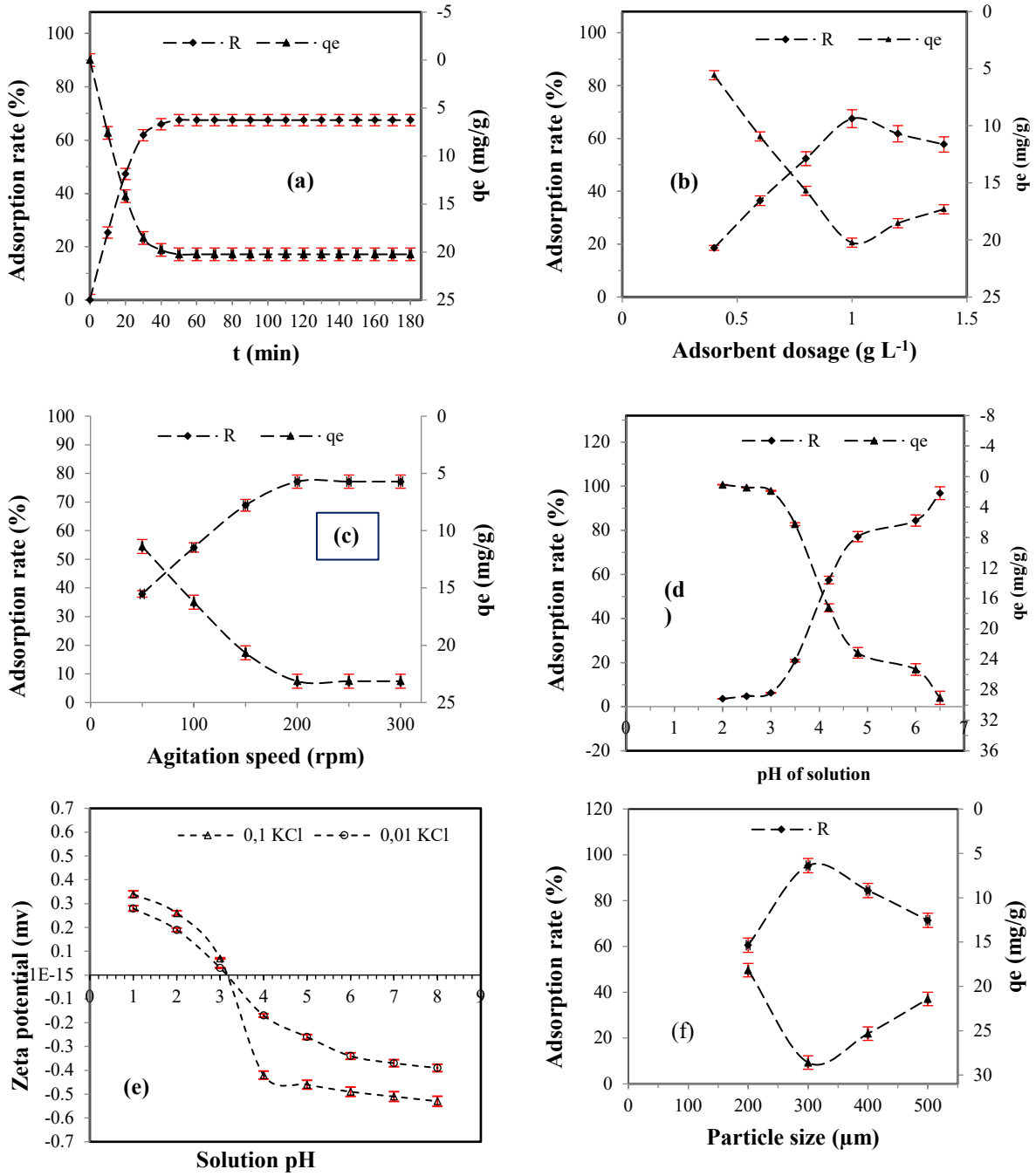

Figure 2 Plots of (a) effect of contact time, (b) effect of adsorbent dosage, (c) effect of agitation speed, (d) effect of initial pH, (e) Zeta potential as a function of solution pH and (f) effect of particle size.

4) Effect of agitation speed

The action of stirring speed has a considerable impact on the adsorption process, as it plays a vital role in the diffusion of metal ions from the liquid to the solid surface [18]. In this perspective, we experimented with different stirring speeds from 50 to 250 rpm (Figure 2c). From Figure 2c, it was observed that the adsorption efficiency gradually progressed at speeds between 50 and 200 rpm. the adsorption yield and capacity increased by 11.76 mg g^{-1} and 39.2%, respectively, in this interval. On the other hand, we noticed that the removal of cadmium is maintained constantly above 200 rpm (R = 77.13%). The good propagation of adsorbent particles in the adsorbate as well as the increase in the diffusion coefficient are unquestionably responsible for the adsorption efficiency [14, 36]. The stability of the adsorption process was certainly caused by the cessation of external diffusion and, thus, the removal of the liquid barrier to mass diffusion [16].

5) Effect of initial pH

The pH of the solution is a key element in these processes, particularly with regard to the adsorption of metal ions on a solid. For this approach, we experimented with a pH variation from 2 to 10. The determination of the zero charge point (PZC) experimentally is shown in Figure 2e, and the effect of pH on cadmium adsorption is shown in Figure 2d.

From the experimental results, we observed that the pH value indicating the PZC is 3.2. The experimental results obtained confirmed the existence of a positive correlation between cadmium ions and modified slag (MS) at pH below 3.2. Indeed, we noticed that the rate and capacity of cadmium adsorption in solution increased significantly at pHs between 3.4 and 6 (Figure 2d). This development is very coherent since the surface of the slag in these environments is negatively charged. From this result, we deduced that the adsorption of cadmium ions took place under the effect of electrostatic attraction [37–38]. At pH < pHpzc, the positively charged adsorbent surface prevented cadmium adsorption due to electrostatic repulsion, which reduced the adsorption rate and capacity [38]. In addition, excess protons hinder the movement of cadmium from solution to the adsorbent surface [13].

This is completely normal, since there is an association between adsorption and chemical precipitation [15]. It is important to emphasize that cadmium begins to precipitate in the form of oxide from pH 6.1 [39]. For this purpose, we chose pH = 6 as the optimal value. According to the bibliography, similar studies (optimal adsorption at pH = 6) have been cited [40–43].

6) Effect of particle size

The influence of particle size on the performance of cadmium adsorption on MS is presented in Figure 2f. From experimental data, it was observed that the cadmium sorption was best at Øs = 300 µm. The calculated adsorption rates at 500, 400, 300, and 200 µm were 71.4%, 84.43%, 95.3%, and 67.4%, respectively. The reduction in particle size from 500 to 300 µm caused an increase in the adsorption surface area, which generated an increase in adsorption efficiency [14, 44]. It is important to mention that the adsorption process decreased for Øs = 200 µm (Figure 2f). This effect could be clarified by the phenomenon of coalescence, that is to say the return to larger diameters. [18, 36]. These tests allowed us to predict that the adsorption rate at different particle sizes is controlled by intraparticle diffusion. It is important to indicate that this phenomenon is controlled by the relationship between the surface of the adsorbent and the volume of the adsorbate, that is to say the surface/volume ratio. The larger the surface area, the more effective the adsorption [45].

7) Effect of initial concentration

In order to represent the experimental adsorption isotherm and measure the optimal adsorption capacity, we examined the impact of the initial concentration of cadmium ions, see Figure 3a.

The tests performed indicated that the adsorption capacity went through two stages. First, it increased from 30 to 240 mg L^{-1}, then it became stable despite the increase in the initial concentration from 240 to 300 mg L^{-1} (Figure 3a). The increase in the initial concentration created a strong driving force facilitating the transport of cadmium ions from the solution to the adsorbent by reducing the resistance to mass transfer [17, 46]. The invariability of the maximum capacity was certainly caused by the saturation of the surface of the adsorbent and also the elimination of resistance to external diffusion.

In Figure 3a, it was also observed that the sorption efficiency of cadmium decreased with the increase in the initial concentration. Indeed, the supply of cadmium ions relative to a limited number of free sites accelerates saturation, which leads to a weakening of the adsorption rate [6, 19]. The experiment carried out led us to conclude that the maximum adsorption capacity in our experimental conditions is 133.34 mg g^{-1}.

8) Adsorption isotherms

The adsorption isotherms were developed to determine the quantities adsorbed at equilibrium and also to identify the reacting interactions for an adsorbate adsorbent system. For this purpose, we opted for the Freundlich, Langmuir, and Temkin models to elucidate

this phenomenon, namely the adsorption of cadmium on MS. The Freundlich model was used to describe the adsorption process on heterogeneous surfaces in a reversible system. Its linear form is represented by Eq. 3 [29].

$$logq_e = logk + \frac{1}{n} logC_e \quad \text{(Eq. 3)}$$

The Langmuir model was used to describe the adsorption process on a single energetically homogeneous layer, where the equivalent adsorption sites can only contain one molecule per site. Its linear equation and the equation determining the separation factor (RL) are represented by Eq. 4 and 5 [17].

$$\frac{C_e}{q_e} = \frac{1}{q_{max}} C_e + \frac{1}{q_{max} b} \quad \text{(Eq. 4)}$$

$$R_L = \frac{1}{1+C_0 b} \quad \text{(Eq. 5)}$$

The Temkin model was established on the principle that the heat of adsorption of molecules located on the same layer decreases linearly due to the strengthening of the surface coverage of the adsorbent. Its linear equation is represented by Eq. 6 [7].

$$qe = B_T lnA_T + B_T lnCe \quad \text{(Eq. 6)}$$

Where q_e and q_{max} are equilibrium adsorption capacity and maximum capacity (mg g^{-1}), C_0 and C_e are the initial concentrations and at equilibrium (mg L^{-1}), b is the thermodynamic constant of Langmuir (L.mg^{-1}), R_L: the ratio indicates the quality of the adsorption, k_F and 1/n are the Freundlich constants related to adsorption and affinity, $B_T = \frac{RT}{b_T}$, A_T is Temkin isotherm equilibrium binding constant (L g^{-1}), bT is constant related to heat of sorption (KJ $kmol^{-1}$).

The plots of the Freundlich, Langmuir and Temkin models are reproduced in Figures 3b, 3c, and 3d. The appearance of the adsorption isotherms is represented in Figure 3e. The values of their parameters are displayed in Table 2. The correlation coefficients and parameters of the models examined, namely the Freundlich, Langmuir and Temkin models were determined from Figures 3b, 3c and 3d, respectively.

Based on the results presented in Table 2, it was found that the Langmuir model is best suited to the experimental data. Indeed, the correlation coefficient of the Langmuir model is higher than that of other models ($R^2_{Lang.} > R^2_{Temk.} > R^2_{Freu.}$). Moreover, the maximum experimental and theoretical adsorbed quantities are very similar.

Table 2 Isotherm parameters for cadmium adsorption

Models	Parameters	Values
Freundlich	k_F (mg g^{-1})(mL mg^{-1})$^{1/n}$	22.64
	n	3.07
	R^2	0.927
Langmuir	q_{max} (mg g^{-1})	134.06
	k_L (L mg^{-1})	0.128
	R^2	0.999
	R_L	0.23-0.02
Temkin	b_T (kJ mol^{-1})	0.73
	A_T (L g^{-1})	2.01
	R^2	0.941

From Figures 3a and 3e, we observed that the Langmuir and experimental isotherm plots are very consistent, which confirms that the adsorption of cadmium on MS was performed on a monolayer and homogeneous surface [3, 7]. Indeed, it has been observed that the adsorption isotherm of Langmuir and type L. It passes through a rapid phase in the domain of low concentrations, then a moderately weak phase, and ends in a constant phase with the appearance of a long horizontal plateau. This effect tells us about the formation of a monolayer [15–17].

From Table 2, it was also noticed that the values of the Freundlich parameter ($0 < n < 10$) and the separation factor ($0 < R_L < 1$) confirmed the favorable nature of the adsorption process [5, 15, 45]. The value of the Temkin model parameter (b_T) indicated that the adsorption is physical ($b_T < 8$ kJ mol^{-1}) [3, 18]. It is essential to emphasize that the adsorption on BFS and MS was performed on a homogeneous monolayer surface [19–21].

9) Kinetics of adsorption

The reaction speed of the process was studied using pseudo-first-order (PFO) and pseudo-second-order (PSO) models (Eq. 7 and 8) [11, 21]. The mechanism of cadmium transfer from solution to MS surface was examined by external diffusion (ED) and internal diffusion (ID) models (Eq. 9 and 10) [23, 47].

$$\log(q_e - q) = -k_L t + logq_e \quad \text{(Eq. 7)}$$

$$\frac{t}{q} = \frac{1}{k_B q_e^2} + \frac{t}{q_e} \quad \text{(Eq. 8)}$$

$$q = k_I \sqrt{t} + C_{Int} \quad \text{(Eq. 9)}$$

$$logC_t = k_E t + C_{Ext} \quad \text{(Eq. 10)}$$

where Ct is the concentration at time t (mg L^{-1}), q is the quantity adsorbed at time t (mg g^{-1}), q_e is the adsorbed quantity at equilibrium (mg g^{-1}), t is the time

of adsorption process, k_L is the constant of pseudo-first-order model (min^{-1}), kB is the constant of pseudo second order model (g mg^{-1} min), k_E is the film diffusion coefficient (min^{-1}); k_I is the diffusion rate constant in the pores (mg m^{-1} $min^{½}$) and C_{Int} and C_{Ext} are the intercepts.

The graphical presentations from equations 7 to 10 are reproduced in the Figure 4 and their parameters are reported in Table 3. The modeling results indicated that the correlation coefficients of the pseudo-second-order model ($R^2 \geq 0.99$) are higher than those of the pseudo-first-order model ($R^2 \leq 0.94$) (Table 3). Furthermore, it was observed that the experimental maximum capacities and the resulting theoretical maximum capacities of the pseudo-first-order model are almost identical (Table 3). From these results, it was established that cadmium adsorption on MS follows pseudo-second-order kinetics [21, 38].

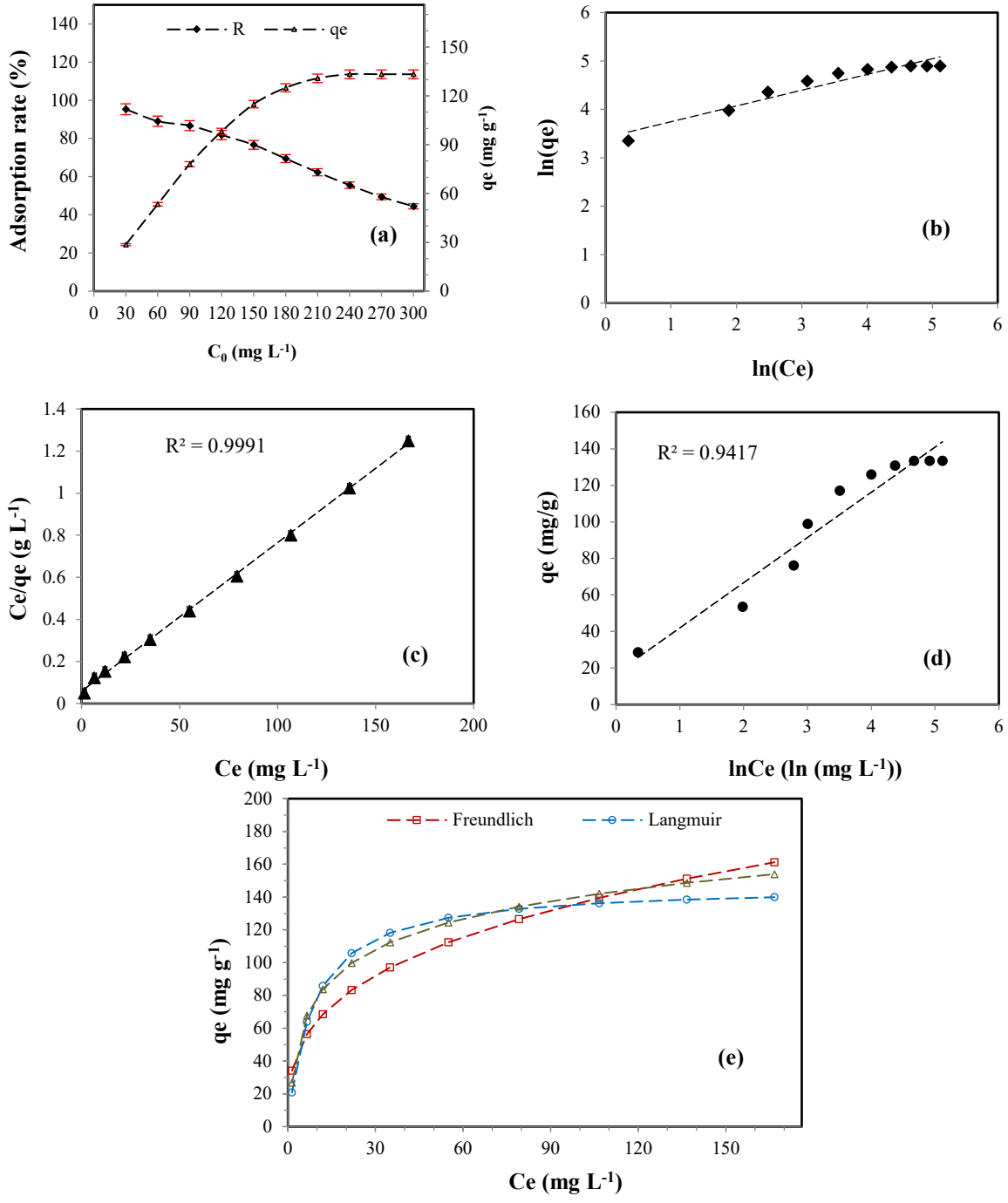

Figure 3 Plots of (a) effect of initial concentration on cadmium adsorption, (b) presentation of the Freundlich model, (c) presentation of the Langmuir model, (d) presentation of the Temkin model and (e) presentation of cadmium adsorption isotherms on MS.

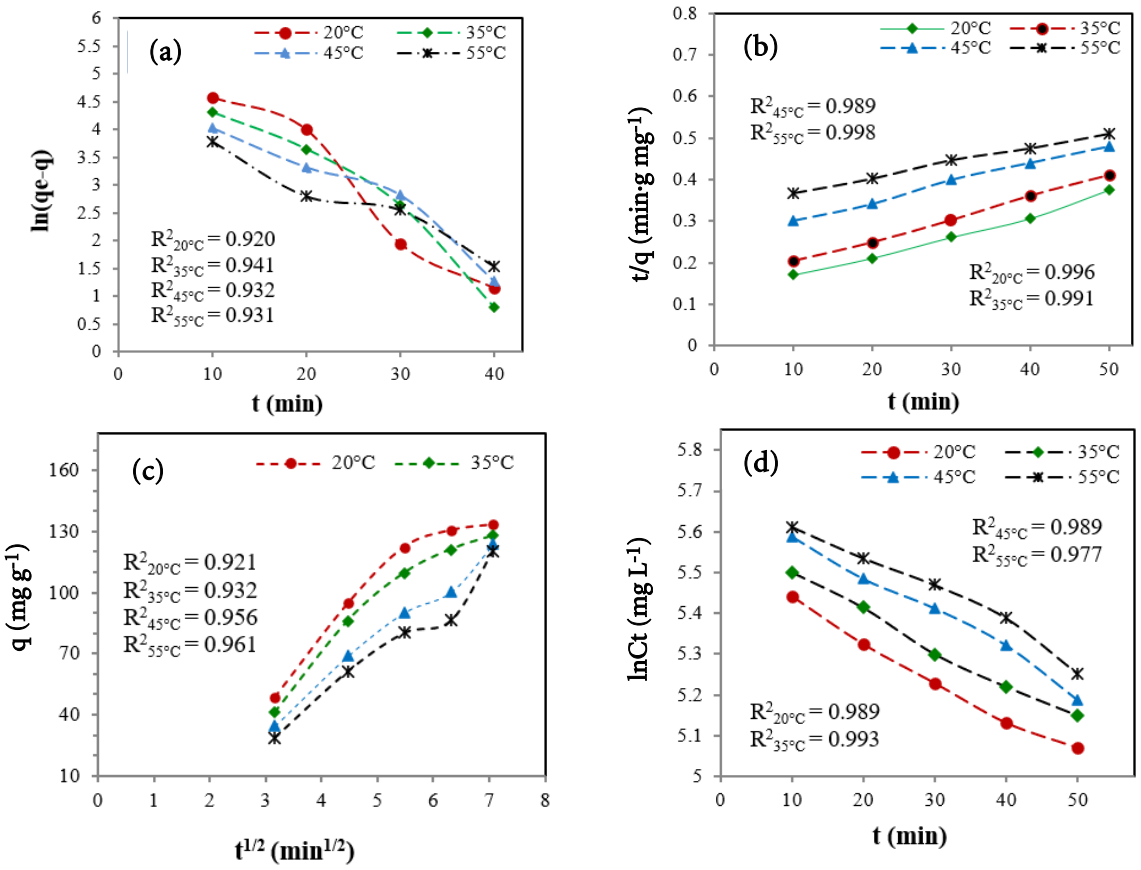

Figure 4 Plots of (a) PFO, (b) PSO, (c) ID and (d) ED.

Table 3 Kinetic parameters

Models	Parameters	Values			
	T (°C)	20	35	45	55
	qe_{exp} (mg g^{-1})	134.34	127.81	123.78	120.31
PFO	K_L (min^{-1})	0.328	0.304	0.291	0.281
	qe_{theo} (mg g^{-1})	145.89	136.14	131.34	127.65
	R^2	0.92	0.941	0.932	0.931
PSO	K_B (g/mg min)	0,0045	0,0056	0,0066	0,0074
	qe_{theo} (mg g^{-1})	134.92	128.42	124.33	121.08
	R^2	0.996	0.991	0.989	0.998
ED	C_{ext}	5.52	5.58	5.65	5.68
	K_{ext} (min^{-1})	0.0093	0.0082	0.0071	0.0062
	R^2	0.989	0.993	0.989	0.977
ID	C_{int}	11.2	20.36	29.64	40.85
	K_{int} (mg g.min^{-1})	20.34	11.35	6.46	4.52
	R^2	0.921	0.932	0.956	0.961

From the resulting graph of Eq. 9, it was observed that the lines were not linear and did not pass through the origin. Moreover, it was displayed in Table 3 that the correlation coefficients were greater than 0.9. Based on these data, we established that intraparticle diffusion is not the only mechanism regulating the cadmium adsorption process on MS [19, 47]. On the other hand, the plots resulting from Eq. 10 showed linear lines with correlation coefficients of more than 0.95 (Figure 3d and Table 3). From this information, it was revealed that external diffusion also controlled the transfer of cadmium ions to the adsorbent [3, 17–18].

From these achievements, we could conclude that the adsorption process of cadmium on MS is controlled sequentially by external and internal diffusion [3, 15]. It should be noted that with the rise in temperature, the thickness of the film widened, which caused a slow diffusion of cadmium ions towards the MS [49]. It is for this reason that we observed a clear regression in the value of the diffusion constant (kw) (Table 3).

10) Effect of temperature

The kinetics of the adsorption of cadmium in solution under the effect of temperature are shown in Figure 5a. The test results showed that the efficiency of cadmium adsorption on MS decreased with the temperature of the medium. Indeed, it was noted that the optimal capacity and the adsorption rate declined, respectively, by 8.44 mg g^{-1} and 28.13% between 20 and 55 °C. From this action, we deduced that the adsorption of cadmium on MS is exothermic [16–17]. The weakening of the adsorption process with the increase in temperature was surely caused by the progression of the movements of the cadmium ions in solution, which attenuated the correlation between adsorbent and adsorbate [49].

In the same perspective, a thermodynamic examination was undertaken to identify the nature and mechanisms of interaction recommending this process. The nature of the adsorption process was identified by the values of the thermodynamic parameters, namely ΔG°, ΔH°, and ΔS°. These parameters were calculated from Eq. 11–13 [13, 35]. The interaction mechanism favoring the adsorption of cadmium was verified by the value of the activation energy. The Arrhenius equation (Eq. 14) was used to calculate the activation energy [6].

$$\Delta G^0 = -RT\ln k_d \quad \text{(Eq. 11)}$$

$$\ln k_d = \frac{\Delta H^0}{R} \times \frac{1}{T} + \frac{\Delta S^0}{R} \quad \text{(Eq. 12)}$$

$$k_d = \frac{C_i - C_e}{C_e} \times \frac{V}{M} = \frac{q_e}{C_e} \quad \text{(Eq. 13)}$$

$$\ln k_{ap} = \ln A - \frac{E_a}{RT} \quad \text{(Eq. 14)}$$

The apparent constant k_{ap} was evaluated from Eq. 15 [6].

$$k_{ap} = k_L \times K_B \quad \text{(Eq. 15)}$$

Where ΔG° is the Gibbs free energy (kJ mol^{-1}), ΔS° is entropy (J mol^{-1} K^{-1}), ΔH° is enthalpy (kJ mol^{-1}), R is the universal gas constant (8.314 J mol^{-1} K^{-1}), T is the absolute temperature (K) and K_d is distribution coefficient (L g^{-1}), Ea is activation energy, k_L and k_B are the constants of the pseudo first and second order respectively, T is the absolute temperature (K) and A is frequency factor.

Van't Hoff and Arrhenius plots are represented by Figures 5b and 5c. The values of the thermodynamic parameters, activation energy and distribution coefficient are displayed in Table 4.

From Figure 5b, it was observed a good correlation between the Van't Hoff model and the experimental data (R^2: 0.99) (Table 4). The regression of the distribution coefficient (K_d) with the increase in temperature clarified that the cadmium adsorption was less favorable in heated aqueous media [19]. The ΔG°, ΔH°, and ΔS° values indicate that the adsorption process accomplished was spontaneous, exothermic, and less entropic [16, 35] (Table 5). A regression of ΔG° with increasing solution temperature demonstrated that mass transfer is inversely proportional to the temperature of the medium [13]. The enthalpy value ($\Delta H° \leq 40$ kJ mol^{-1}) explained that the removal of cadmium was accomplished by physical adsorption [9, 17]. This aspect was also endorsed by the values of Gibbs energy ($-20 < \Delta G° < 0$ kJ mol^{-1}) [14]. The decrease in random movements on the surface of the adsorbent was imposed by the cationic interaction of the cadmium ions with the slag examined [23]. The energy value of activation (Table 4) confirmed that the cadmium adsorption process of MS is carried out physically [3].

11) Cadmium desorption

In order to facilitate the desorption of cadmium from the saturated MS. We propose acidic eluents with the aim of modifying the charges of the adsorbent surface and thus intensifying the repulsive effect. The equation below (Eq. 16) was used to assess the desorption quality.

$$desorption\ rate = \frac{q_{des}}{q_{ads}} \times 100 \quad \text{(Eq. 16)}$$

Where q_{ads} is the adsorbed quantity at equilibrium (mg g^{-1}) for cycle I and q_{des} is the desorbed quantity at equilibrium (mg g^{-1}) of each cycle.

The kinetics and efficiency of cadmium desorption under the effect of various solutions are reproduced in Figures 6a. From the experimental data, it was noticed that the presence of HCl in solution strongly promoted the desorption of cadmium ions from the saturated MS. Indeed, the desorption rate of cadmium was largely high under the action of HCl and too little under the action of distilled water ($HCl > H_2SO_4 > HNO_3 > H_2O$) (Figure 6(a)). The observed efficiency was probably caused by the generation of a large number of protons, which influenced the character of the adsorbent surface [3, 9]. According to the experimental acquired, it was also specified that the saturated MS could be reused for five successive cycles using HCl (0.1M) (Figure 6b). The inefficiency of the desorption process after the fifth cycle was undoubtedly generated by the loss of mass and the depletion of active adsorption sites [15, 17].

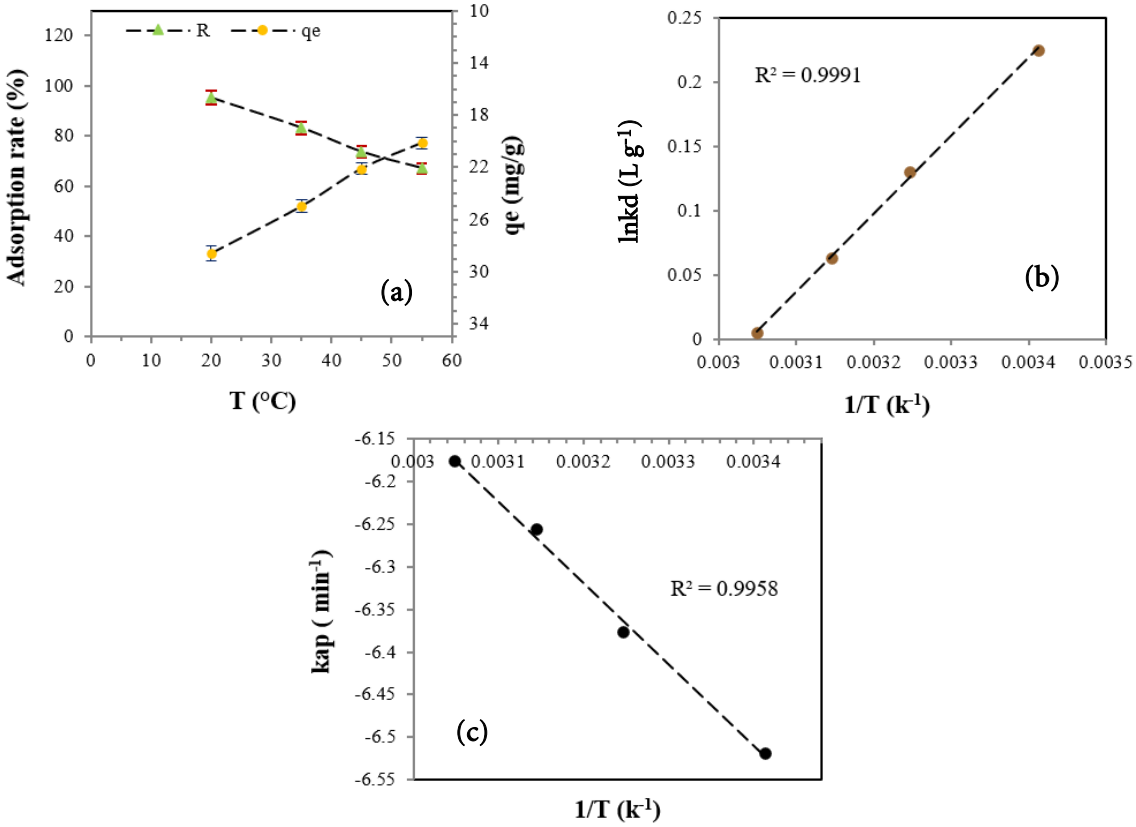

Figure 5 Plots of (a) Effect of temperature, (b) Van't Hoff equation and (c) Arrhenius equation.

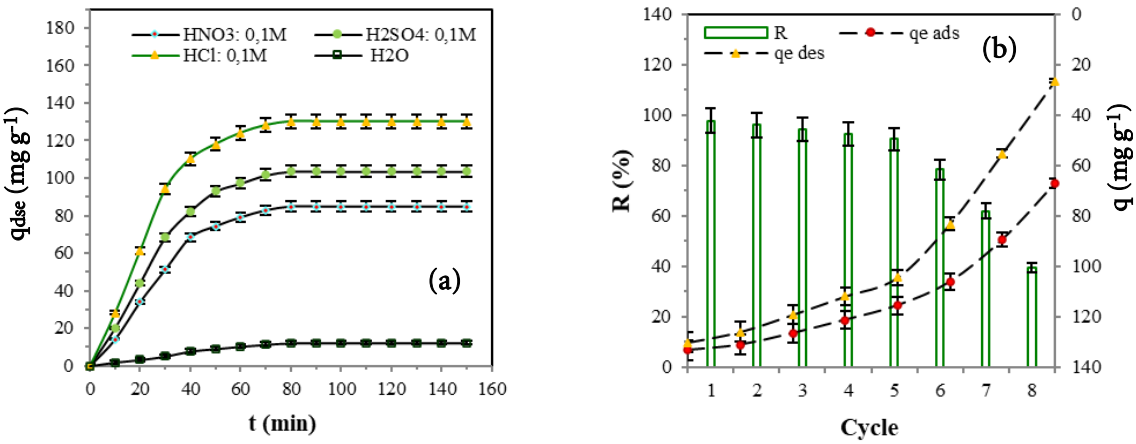

Figure 6 Plots of (a) desorption kinetics and (b) desorption cycles.

Table 4 Thermodynamic parameters of cadmium adsorption

T (K)	ΔH° (kJ mol^{-1})	ΔG° (kJ mol^{-1})	ΔS° (J mol^{-1} K^{-1})	Ea (kJ mol^{-1})	R^2	Kd (L g^{-1})
293	-6.98	-17.42	-25.67	5.07	0.99	1,252
308		-18.07				1,139
318		-18.48				1,065
328		-18.91				1,005

Conclusion

In this study, the adsorption of cadmium ions in batch mode on blast furnace slag converts hydroxy-apatite-zeolite was discussed. The transformation was carried out by adding alkaline chemical reagents and performing heat treatment. The studies conducted revealed that the MS mainly consisted of sodium oxide, silica, phosphorus pentoxide, alumina, and lime. Its PZC was detected at pH 3.2, and its specific surface area is 410.23 m^2 g^{-1}. According to the experimental results, it was discovered that the efficiency of cadmium adsorption on MS essentially depended on the involve-

ment of the determining parameters, namely contact time (50 min), stirring speed (200 rpm), dosage of the adsorbent (1g L^{-1}), pH (6), temperature (20°C), particle size (300 µm), and initial concentration (240 mg L^{-1}). Its maximum adsorption capacity was 133.34 mg g^{-1}. The adsorbent-adsorbate interaction study indicated that the Langmuir model (R^2: 0.99; qmax: 134.06 mg g^{-1}) is the most commonly adopted to describe cadmium adsorption on MS, thus indicating monolayer adsorption on homogeneous active sites. The para-meters RL (0.02–0.23) and n (3.07) from the models examined revealed that adsorption is favorable. The kinetic study showed that the cadmium adsorption on MS follows pseudo-second-order kinetics (R^2: 99). In addition, it revealed that the transport of cadmium from the solution to the adsorbent surface of MS was controlled by external and intraparticle diffusion. The thermodynamic parameters ΔG°, ΔH°, and ΔS° explained that cadmium adsorption on MS is spontaneous, exothermic, and less entropic, respectively. The values of the enthalpy (ΔH°: -6.98 kJ mol^{-1}) and the activation energy (Ea: 5.07 kJ mol^{-1}) revealed that this process was accomplished physically under the effect of electro-static attraction. The desorption process explained on the one hand that HCl (0.1 M) is the most favorable eluent. On the other hand, it was pointed out that MS could be reused for five successive cycles. From this study, we reasoned that hydroxyapatite-zeolite can be exploited as a reliable adsorbent to remove cadmium ions from wastewater.

References

[1] Ul Mehdi, S., Aravamudan, K. Adsorption of cadmium ions on silica coated metal organic framework. Materials Today: Proceedings, 2022, 61, 487–497.

[2] Mansoorianfar, M., Nabipour, H., Pahlevani, F., Zhao, Y., Hussain, Z., Hojjati-Najafabadi, A., …, Pei, R. Recent progress on adsorption of cadmium ions from water systems using metal-organic frameworks (MOFs) as an efficient class of porous materials. Environmental Research, 2022, 214, 114113.

[3] Chouchane, Boukari, A. Impact of influencing parameters on the adsorption of nickel by kaolin in an aqueous medium. Analytical and Bioanalytical Chemistry Research, 2022, 9(4), 381–399.

[4] Uddin, M.K. A review on the adsorption of heavy metals by clay minerals, with special focus on the past decade. Chemical Engineering Journal, 2017, 308, 438–462.

[5] Cui, X., Fang, S., Yao, Y., Li, T., Ni, Q., Yang, X., He, Z. Potential mechanisms of cadmium removal from aqueous solution by Canna indica derived biochar. Science of the Total Environment, 2016, 562, 517–525.

[6] Zhou, F., Ye, G., Gao, Y., Wang, H., Zhou, S., Liu, Y., Yan, C., Cadmium adsorption by thermal-activated sepiolite: Application to in-situ remediation of artificially contaminated soil. Journal of Hazardous Materials, 2021, 423, 127104.

[7] Tan, I.A.W., Chan, J.C., Hameed, B.H., Lim, L.L.P. Adsorption behavior of cadmium ions onto phosphoric acid-impregnated microwave-induced mesoporous activated carbon. Journal of Water Process Engineering, 2016, 1, 60–70.

[8] Semerjian, L., Equilibrium and kinetics of cadmium adsorption from aqueous solutions using untreated Pinus halepensis sawdust. Journal of Hazardous Materials, 2010, 173(1–3), 236–242.

[9] Tasharrofi, S., Rouzitalab, Z., Maklavany, D. M., Esmaeili, A., Rabieezadeh, M., Askarieh, M., …, Taghdisian H. Adsorption of cadmium using modified zeolite-supported nanoscale zero-valent iron composites as a reactive material for PRBs. Science of the Total Environment, 2020, 736, 139570.

[10] Mousakhani, M., Sarlak, N. Electrospun composite nanofibre adsorbents for effective removal of Cd^{2+} from polluted water. Materials Chemistry and Physics, 2020, 256, 123578.

[11] Hussein, T.S., Faisal, A.A.H. Nanoparticles of (calcium/aluminum/CTAB) layered double hydroxide immobilization onto iron slag for removing of cadmium ions from aqueous environment. Arabian Journal of Chemistry, 2023, 16(9), 2023, 105031.

[12] Zemouli, S., Chelghoum, N. Use of ground granulated blast furnace slag in soils stabilization. Review of Science Technology, 2018, 36, 103–114.

[13] Chouchane, T., Khireddine, O., Boukari, A. Kinetic studies of Ni(II) ions adsorption from aqueous solutions using the blast furnace slag (BF slag). Journal of Engineering and Applied Science, 2021, 68, 34.

[14] Chouchane, T., Chibani, S., Khireddine, O., Boukari, A. Adsorption study of Pb(II) ions on the blast furnace slag (BFS) from aqueous solution. Iranian Journal of Materials Science and Engineering, 2023, 20(1), 1–13.

[15] Chouchane, T., Boukari, A., Khireddine, O., Chibani, S., Chouchane, S. Equilibrium, kinetics, and thermodynamics of batch adsorption of Mn(II) ions on blast furnace slag (BFS) and kaolin (KGA). Journal of Engineering and Applied Science, 2023, 70, 58.

[16] Chouchane, T., Boukari, A., Khireddine, O., Chibani, S., Chouchane, S. Cu(II) removal from

aqueous medium using blast furnace slag (BFS) as an effective adsorbent. Eurasian Journal of Chemistry, 2023, 28(2), 110.

[17] Chouchane, T., Khireddine, O., Chibani, S., Boukari, A. Removal of Cr(III), Pb(II) and Cr-Pb mixture by blast furnace slag (BFS) in solution. Analytical and Bioanalytical Chemistry Research, 2023, 10 (3), 251–268.

[18] Li, C.X., Zhang, Q.W., Li, L. Synthesis of NaA zeolite from blast furnace slag (BFS) and its utilization for adsorption of basic dye (methylene blue). Journal of Physics: Conference Series, 2021, 2224, 012068.

[19] Dhmees, A.S., Klaleel, N.M., Mahoud, S.A. Synthesis of silica nanoparticles from blast furnace slag as cost-effective adsorbent for efficient azo-dye removal. Egyptian Journal of Petroleum, 2018, 27, 1113–1121.

[20] Yamaguchi, S., Hongo, T. Synthesis of metaettringite from blast furnace slag and evaluation of its boron adsorption ability. Environmental Science and Pollution Research, 2021, 28, 15070–15075.

[21] Le, Q.T.N., Vivas, E.L., Cho, K. Oxalated blast-furnace slag for the removal of cobalt(II) ions from aqueous solutions. Journal of Industrial and Engineering Chemistry, 2021, 95, 57–65.

[22] Shao, N., Li, S., Yan, F., Su, Y., Liu, F., Zhang, Z. An all-in-one strategy for the adsorption of heavy metal ions and photodegradation of organic pollutants using steel slag-derived calcium silicate hydrate. Journal of Hazardous Materials, 2020, 382, 121120.

[23] Xue, Y., Hou, H., Zhu, S. Adsorption removal of reactive dyes from aqueous solution by modified basic oxygen furnace slag: Isotherm and kinetic study. Chemical Engineering Journal, 2009, 147, 272–279.

[24] Xue, Y., Wu, S., Zhou, M. Adsorption characterization of Cu(II) from aqueous solution onto basic oxygen furnace slag. Chemical Engineering Journal, 2013, 231, 355–364

[25] Li, C., Li, X., Yu, Y., Zhang, Q., Li, L., Zhong, H., Wang, S., novel conversion for blast furnace slag (BFS) to the synthesis of hydroxy-apatite-zeolite material and its evaluation of adsorption properties. Journal of Industrial and Engineering Chemistry, 2022, 105, 63–73.

[26] Piatak, N.M., Seal, R.R., Hoppe, D.A., Green, C.J., Buszka, P.M. Geochemical characterization of iron and steel slag and its potential to remove phosphate and neutralize acid. Minerals, 2019, 9, 468.

[27] Zuo, M., Renman, G., Gustafsson, J.P., Klysubun, W. Phosphorus removal by slag depends on its mineralogical composition: A comparative study of AOD and EAF slags. Journal of Water Process Engineering, 2018, 25, 105–112.

[28] Navarro, C., Dнaz, M., Villa-Garcнa, M.A. Physico-chemical characterization of steel slag. study of its behavior under simulated environmental conditions. Environmental Science & Technology, 2010, 44 (14), 5383–5388.

[29] Basaleh, A.A., Al-Malack, M.H., Saleh, T.A. Poly(acrylamide acrylic acid) grafted on steel slag as an efficient magnetic adsorbent for cationic and anionic dyes. Journal of Environmental Chemical Engineering, 2021, 9, 105126.

[30] Mustapha L.S., Yusuff A.S., Dim P.E. RSM optimization studies for cadmium ions adsorption onto pristine and acid-modified kaolinite clay. Heliyon, 2023, 9(8), e18634.

[31] Naihi, H., Baini, R., Yakub I. Adsorption kinetics and isotherm of cadmium onto NaOH-treated oil palm empty fruit bunch. Biocatalysis and Agricultural Biotechnology, 2022, 45, 102489.

[32] Hussain, N., Chantrapromma, S., Suwunwong, T., Phoungthong, K. Cadmium (II) removal from aqueous solution using magnetic spent coffee ground biochar: kinetics, isotherm and thermo-dynamic adsorption, Materials Research Express, 2020, 7, 085503.

[33] Tan, X., Wei, W., Xu, C., Meng, Y., Bai, W., Yang, W., Lin A. Manganese-modified biochar for highly efficient sorption of cadmium, Environmental Science and Pollution Research, 2020, 27, 9126–9134.

[34] Zhao, Y., Yang, S., Ding, D., Chen, J., Yang, Y., Lei, Z., …, Zhang, Z. Effective adsorption of Cr (VI) from aqueous solution using natural Akadama clay, Journal of Colloid and Interface Science, 2013, 395, 198–204.

[35] Foroutan, R., Mohammadi, R., Farjadfard, S., Esmaeili, H., Ramavandi, B., Sorial, G.A., Eggshell nano-particle potential for methyl violet and mercury ion removal: Surface study and field application. Advanced Powder Technology, 2019, 30, 2188–2199.

[36] Yogeshwaran, V., Priya, A.K. Adsorption of lead ion concentration from the aqueous solution using tobacco leaves. Materials Today: Proceedings, 2021, 37, 486–495.

[37] Foroutan, R., Ahmadlouydarab, M., Ramavandi, B., Mohammadi, R., Studying the physico-chemical characteristics and metals adsorptive behavior of CMC-g-HAp/Fe_3O_4 anobiocomposite. Journal of Envi-

ronmental Chemical Engineering, 2018, 6, 6049–6058.

[38] Shi, T., Xie, Z., Zhu, Z., Shi, W., Liu, Y., Liu, M., Mo, X. Effective removal of metal ions and cationic dyes from aqueous solution using different hydrazine–dopamine modified sodium alginate. International Journal of Biological Macromolecules, 2023, 195, 317–328.

[39] Baghban, E., Mehrabani-Zeinabad, A., Moheb, A. The effects of operational parameters on the electrochemical removal of cadmium ion from dilute aqueous solutions. Hydrometallurgy 2014, 149, 97–105.

[40] Zhou, X., Zhou, J., Liu, Y., Guo, J., Ren, J., Zhou, F. Preparation of iminodiacetic acid-modified magnetic biochar by carbonization, magnetization and functional modification for Cd(II) removal in water. Fuel, 2018, 233, 469–479.

[41] Liu, C., Ye, J., Lin, Y., Wu, J., Price, G.W., Burton, D., Wang, Y. Removal of Cadmium (II) using water hyacinth (Eichhornia crassipes) biochar alginate beads in aqueous solutions. Environmental Pollution, 2020, 264, 114785.

[42] Tao, Q., Chen, Y., Zhao, J., Li, B., Li, Y., Tao, S., …, Wang, C. Enhanced Cd removal from aqueous solution by biologically modified biochar derived from digestion residue of corn straw silage. Science of the Total Environment, 2019, 674, 213–222.

[43] Es-sahbany, H., El Hachimi, M.L., Hsissou, R., Belfaquir, M., Es-sahbany, K., Nkhili, S., …, Elyoubi, M.S. Adsorption of heavy metal (cadmium) in synthetic wastewater by the natural clay as a potential adsorbent (Tangier-Tetouan-Al Hoceima – Morocco region). Materials Today: Proceedings, 2021, 45, 7299–7305.

[44] Chouchane, T., Yahi, M., Boukari, A., Balaska, A., Chouchane, S. Adsorption of the copper in solution by the kaolin. Journal of Materials and Environmental Science, 2016, 7(8), 2825–2842.

[45] Wekoye, J.N., Wanyonyi, W.C., Wangila, P.T., Tonui, M.K. Kinetic and equilibrium studies of Congo red dye adsorption on cabbage waste powder. Environmental Chemistry and Ecotoxicology, 2020, 2, 24–1.

[46] Alizadeh, N., Salimi, A. Simultaneous adsorption and catalytic degradation of methylene blue dye over recyclable $Mn_4(P_2O_7)_3$ nanoflakes: Mechanism and efficiency, Environmental Nanotechnology, Monitoring & Management, 2023, 20, 100806.

[47] Labidi, N.S. Adsorption kinetics of basic blue-41 dye on synthetic foam-shaped zeolite ZSM-5. Iranian Journal of Materials Science and Engineering, 2022, 19(1), 1–8.

[48] Gurses, A., Hassani, A., Kiransan, M., Acisli, O., Karaca, S. Removal of methylene blue from aqueous solution using by untreated lignite as potential low-cost adsorbent: kinetic, thermodynamic and equilibrium approach. Journal of Water Process Engineering, 2014, 2, 10–21.

[49] Karami, K., Beram, S.M., Bayat, P., Siadatnasab, F., Ramezanpour, A. A novel nanohybrid based on metal–organic framework MIL101-Cr/PANI/Ag for the adsorption of cationic methylene blue dye from aqueous solution. Journal of Molecular Structure, 2022, 1247, 131352.